

# Electrochemical oxidation of acidic Alberta coal slurries

G. THOMAS\*, M. CHETTIAR, V. I. BIRSS†

Department of Chemistry, The University of Calgary, 2500 University Drive N.W., Calgary, Alberta T2N 1N4, Canada

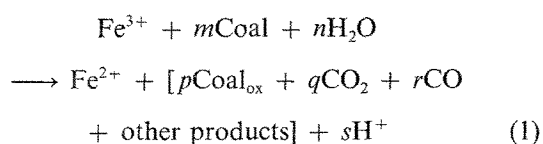
Received 16 December 1989; revised 12 January 1990

The electrochemical oxidation of four different types of Alberta coals of bituminous and sub-bituminous rank have been studied in 1 M H<sub>2</sub>SO<sub>4</sub> slurries at 90°C under potentiostatic conditions at an applied potential of 1.0 V with respect to RHE. Two particle sizes (> 200 and < 60 mesh) were used to determine the rate constant for the electrochemical oxidation of coal mediated by Fe<sup>3+</sup>. Two rate constants,  $k_{c,1}$  and  $k_{c,2}$ , representing initial (0–~6 h) and subsequent (~6–24 h) stages of electrochemical oxidation of coal, respectively, were observed. A correlation between the rate constants and the fixed carbon content (rank) of the coals was drawn. Gas chromatographic analysis of the gaseous oxidation products indicated the production of carbon dioxide. The rate and current efficiency for this production was determined as a function of electrolysis time with the rate of production reaching a steady-state level after a few hours of electrolysis. Possible mechanisms for the oxidation of coal are discussed, based on structural and functional group models.

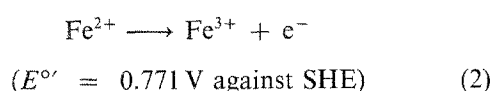
## 1. Introduction

In recent years, there has been a significant amount of interest in the development of new models of coal utilization and methods of coal conversion. The feasibility of using electrochemical methods for the conversion of coal to various products was first tested in alkaline solutions [1–4], while the oxidation of acidic coal slurries to commercially useful products was first proposed by Coughlin and Farooque in 1979 [5–8]. It was indicated from their results that Fe<sup>3+</sup> ions, which are released from the coal in these acidic slurries, are involved in the oxidation of coal. Further studies of the electrochemical oxidation of coal in acidic slurries by numerous workers [9–15] have clarified the fact that Fe<sup>2+</sup> is oxidized at the anode to Fe<sup>3+</sup>, which in turn mediates the oxidation of coal in the slurry, while hydrogen is produced at the cathode. The overall process can be represented by Reactions 1 to 3, where  $m$ ,  $n$ ,  $p$ ,  $q$ ,  $r$  and  $s$  are coefficients having values which depend on the experimental conditions, and Coal<sub>ox</sub> depicts the oxidized coal products which remain attached to the coal surface.

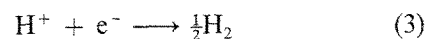
In the slurry



At the anode



At the cathode



The electrochemical oxidation of coal in redox mediator-containing acidic slurries (Reaction 2) has a number of very important advantages. First, Reactions 1 to 3 show that, for two Fe<sup>2+</sup> to Fe<sup>3+</sup> conversions, one molecule of hydrogen gas is produced at the cathode. Since the oxidation of Fe<sup>2+</sup> at platinum occurs at a significantly lower potential than does oxygen evolution, a cell voltage substantially lower than that necessary for conventional water electrolysis leads to the production of hydrogen at a reasonable rate. As the Fe<sup>2+</sup> can be regenerated by the coal (Reaction 2), a sustained production of hydrogen gas can be achieved by the coal oxidation process. Therefore, since hydrogen is a highly desirable commodity, and as it can be produced inexpensively by this route, the electrochemical oxidation of coal is an extremely attractive process.

A second important feature of the electrochemical oxidation of coal is that the gases which are produced during coal oxidation by Fe<sup>3+</sup> in H<sub>2</sub>SO<sub>4</sub> slurries, such as CO<sub>2</sub> and CO, are of very high purity. Any sulphur present in the coal is retained in solution as sulphate, rather than evolving as H<sub>2</sub>S or SO<sub>2</sub>.

Thirdly, it has been reported that a range of liquid products can also be obtained by the electrochemical oxidation of lignite coals in acidic slurries [16]. Organic compounds having carbon chain lengths in the range of C<sub>8</sub> to C<sub>32</sub> have been found in sulphuric acid solutions after electrochemical coal slurry oxidation [16].

These very positive features of the electrochemical

†To whom correspondence should be addressed

\*Present address: Moli Energy Limited, 3958 Myrtle Street, Burnaby, British Columbia, Canada, V5C 4G2.

oxidation of coal have prompted numerous investigators to pursue the process further. The majority of the prior studies have been concerned with various lignite coals [5, 7–9, 13, 16, 17]. The results of these studies have shown that the primary coal product is  $\text{CO}_2$ , with some liquid products also being obtained [5, 16]. Also, it has been reported that the electrochemical activity of the coal diminishes with time of oxidation. This has been suggested to be due to the build-up of oxidized organic functional groups on the coal particle surfaces with time [9–13, 15, 17].

To date, Alberta coals have not been examined in terms of their activity towards electrochemical oxidation. As the structure and properties of coal vary significantly with geological origin and geographical location, it was anticipated that Alberta coals might behave differently during electrochemical oxidation than the more commonly studied lignite coals. To the best of our knowledge, only a limited number of electrochemical studies have been carried out in the past with bituminous coals [10–13] as compared to lignite coals.

In this work, we have chosen a number of sub-bituminous and bituminous coals from a relatively narrow geographical part of the Alberta Plains region and have studied their comparative activity towards electrochemical oxidation. A close proximity between the geographical location of coal samples of different types might enable comparison and correlation of the properties of coals with their rank with greater accuracy than when using coals from various geographical regions. Coal rank (ASTM) in the Alberta Plains region ranges from high volatile bituminous C to lignite A. Relatively high oxygen and low sulphur contents are characteristic of these coals, while they show no caking properties [18]. The ash content of these coals ranges from 10 to 14% (w/w).

The results of efforts to determine the overall feasibility of the electrochemical oxidation of acidic slurries of various types of Alberta coals are presented in this paper, along with an attempt to correlate the rates of the electrochemical oxidation of Alberta coals with the rank of the coal. A graphical approach has been developed [19] to obtain kinetic parameters which reflect the activity of the coals to electrochemical oxidation. We have also developed [20] some novel and efficient methods to revitalize the partially oxidized coal to overcome the observed deactivation of coal after prolonged electrochemical oxidation. These studies have also resulted in the discovery of new organic acid reaction media for electrochemical coal oxidation, for example, acetic acid [21], in which coal conversion to soluble, low molecular weight organic compounds is substantially enhanced as compared to the case in  $\text{H}_2\text{SO}_4$  [16] media.

## 2. Experimental details

### 2.1. General experimental approach

The general procedure utilized in this research involved

the addition of  $\sim 6$  g of a particular pre-treated Alberta coal sample to  $\sim 120$  ml of 1 M  $\text{H}_2\text{SO}_4$ , to which known amounts ( $\sim 15$  mM) of  $\text{FeSO}_4$  had been added. At a constant temperature, stirring rate and electrode potential, the current passed through the cell, as  $\text{Fe}^{2+}$  is continuously oxidized to  $\text{Fe}^{3+}$ , was monitored as a function of time. The analysis of the gaseous products was carried out as a function of time of electrolysis, and solution-soluble liquid products were determined after the completion of each experiment.

### 2.2. Electrochemical details

The electrochemical experiments were carried out utilizing standard three-electrode circuitry controlled by a PARC EG&G 175 universal programmer with a PARC EG&G 173 potentiostat, or a 273 potentiostat interfaced to an Apple IIe microcomputer. The long-time electrolysis data were collected and processed with the use of the PARC 332 corrosion software. A HP 7045B X/Y recorder was used to record all other electrochemical data.

The electrolysis experiments were carried out in a three compartment cell (Fig. 1). This design was used in order to avoid contact of the  $\text{Fe}^{2+/3+}$  species with the counter and reference electrodes. Experiments were carried out at room temperature or higher, in which case the temperature was maintained by circulating hot liquid (Permafil) through the outer jacket of the cell from a constant temperature bath circulator (Lauda, model K6).

A high purity platinum foil (Aldrich Chemical Co., 99.99%,  $7\text{ cm}^2$ ) was used as the working electrode (WE), the anode during electrolysis. While a larger area platinum gauze electrode and a reversible hydrogen electrode (RHE) were used as the counter (CE) and reference (RE) electrodes, respectively. The WE was electrochemically cleaned by repeated cycling

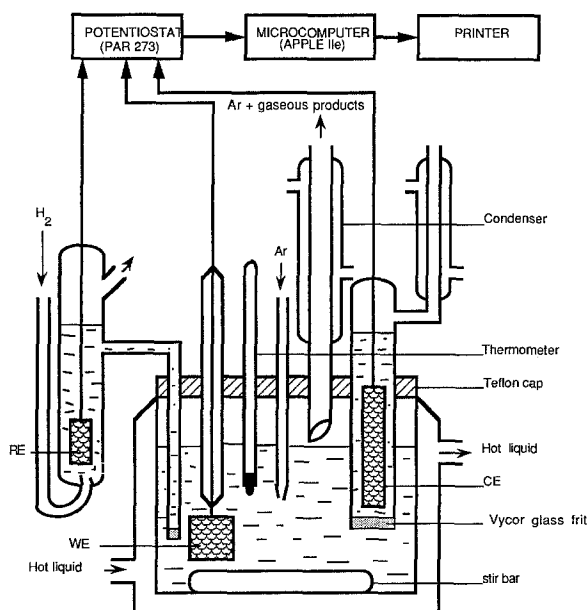


Fig. 1. Schematic diagram of the electrochemical cell.

Table 1. Origin, rank and particle sizes of Alberta coals

Sample type*	Geological formation	ASTM rank <sup>†</sup>	Particle size	
			mesh	$\mu\text{m}$
Luscar-Sterco Coal Valley	Mynheer/Valdor	hvB C	{ > 200 48-64	< 65 250-350
Highvale	Paskapoo	Sb B	{ > 200 48-64	< 65 250-350
Antelope-Bow City (Brooks)	Oldman	Sb B	{ > 200 48-64	< 65 250-350
Vesta (Central Battle River)	Horseshoe/Canyon	Sb C	{ > 200 48-64	< 65 250-350

\* Samples collected from Alberta Plains Coal Region:

<sup>†</sup> Sb = sub-bituminous, hvB = high volatile bituminous.

of its potential between 0.0 and 1.7 V before each experiment.

In all the experiments, the solution was continuously deaerated by bubbling high purity argon gas through the solution at a controlled rate. The coal slurry was stirred at a reproducible rate during each experiment using a large Teflon-coated stirrer bar driven by a magnetic stirrer. This was done in order to keep the coal particles in suspension and also as stirring is required to control the rate of mass transport of  $\text{Fe}^{2+}$  to the WE surface. The reproducibility of stirring was confirmed by the closeness of the data for identical experiments carried out on different days.

### 2.3. Solutions and chemicals

AristraR grade sulphuric acid (BDH) was used together with triply distilled water to make up the sulphuric acid solutions. Analytical grade  $\text{FeSO}_4 \cdot 7\text{H}_2\text{O}$  was used as the source of  $\text{Fe}^{2+}$ . All water was triply distilled. The coal samples were obtained from the Department of Coal and Hydrocarbon Processing (Alberta Research Council, Edmonton, Alberta, Canada). The origin (sample type), geological formation, rank and particle size of these coal samples are given in Table 1.

### 2.4. Pre-treatment of coal

Coal samples were subjected to a careful pre-treatment process before using them in the electrolysis experiments. This was done in order to leach out all of the inorganic matter (ash) from the coal, particularly any Fe-containing species, and to achieve a reproducible chemical and physical condition of the coal. Coal samples were introduced into 1 M  $\text{H}_2\text{SO}_4$  and agitated at 25°C for ~24 h. The sample was then filtered and again subjected to the same washing process. The sample was then refluxed (95 to 97°C) in 1 M  $\text{H}_2\text{SO}_4$  for ~24 h, cooled and then filtered. It was then refluxed again in 1 M  $\text{H}_2\text{SO}_4$  for another 24 h, cooled and filtered. The coal sample was then washed free of acid by repeated agitation in triply distilled water,

filtered and dried under vacuum over anhydrous  $\text{CaSO}_4$  at room temperature and stored in a refrigerator.

### 2.5. Product analysis

The gaseous products obtained from the anode compartment during electrolysis were analyzed with a Shimadzu 8A gas chromatograph (GC) fitted with a carbosieve SII column and a Shimadzu C-R1B Chromatopac integrator. The gaseous products were flushed out of the cell with argon gas and were collected continuously by displacement of 1 M  $\text{H}_2\text{SO}_4$  in a large collection tube. Gas samples were periodically withdrawn from the tube and injected into the GC. After each sampling, the remaining gas in the collection tube was removed in order to ensure the collection of fresh gas from the cell for the next analysis. The total amount of gaseous products could be determined from the periodic GC analysis of the contents of the collection tube together with the measured total volume of gas released from the cell in the experiment.

## 3. Results and discussion

### 3.1. Electrochemistry of $\text{Fe}^{2+/3+}$ (no coal) in 1 M $\text{H}_2\text{SO}_4$

The electrochemical behaviour of the  $\text{Fe}^{2+/3+}$  couple, utilized in the oxidation of coal in most of this work, was examined initially at a platinum WE in 1 M  $\text{H}_2\text{SO}_4$  at various solution stirring rates. A typical voltammogram, obtained at a potential sweep rate of  $20 \text{ mV s}^{-1}$  in a partially oxidized  $\text{FeSO}_4$  solution, is shown in Fig. 2. From the magnitude of the anodic (oxidation) and cathodic (reduction) limiting currents, the concentration of  $\text{Fe}^{2+}$  and/or  $\text{Fe}^{3+}$  could be determined in an electrolysis experiment at any time.

When the potential is held in the range of diffusion limited current plateau, for example at 1.0 V in Fig. 2, it is known [22] that the limiting current ( $I_{lim}$ ) should decrease exponentially with time for a simple diffusion controlled process, as  $\text{Fe}^{2+}$  is oxidized to  $\text{Fe}^{3+}$  (Fig. 3,

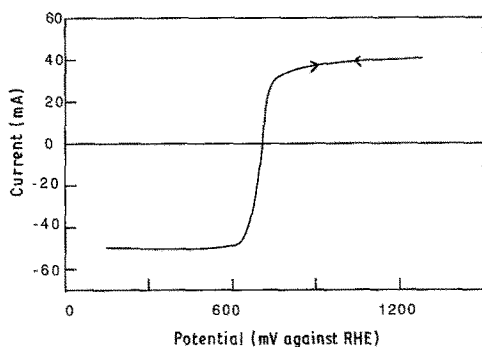


Fig. 2. Voltammogram of partially oxidized 15mM  $\text{FeSO}_4$  at a platinum WE; scan rate =  $20 \text{ mV s}^{-1}$ ;  $T = 25^\circ \text{C}$ .

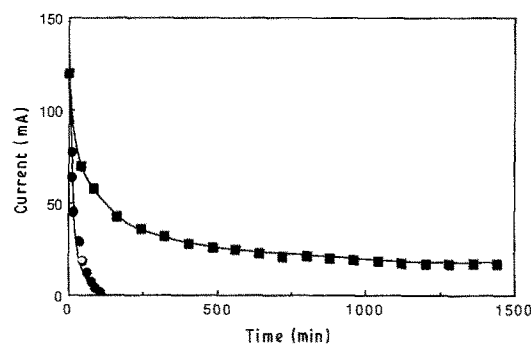


Fig. 4. Current against time response obtained at  $90^\circ \text{C}$  and 1.0 V in 1 M  $\text{H}_2\text{SO}_4$  with a (■) 6 g of Vesta coal (200 mesh) + 15 mM  $\text{FeSO}_4$ ; b (●) 15 mM  $\text{FeSO}_4$  alone (no coal added).

curve a). If the reactant, e.g.  $\text{Fe}^{2+}$ , is being fully regenerated by another reaction (see Reaction 2),  $I_{\text{lim}}$  should remain constant at its original value with time (Fig. 3, curve b). If only a partial regeneration occurs, a decay (Fig. 3, curve c) slower than when no regeneration occurs would be expected [22].

### 3.2. Electrochemical oxidation of acidic coal slurries

**3.2.1. General electrochemical behaviour of Alberta coals.** The electrochemical oxidation of pre-treated Alberta coals was typically carried out at 1.0 V with respect to RHE in 1 M  $\text{H}_2\text{SO}_4$  coal slurries containing known amounts of added  $\text{FeSO}_4$ . The rate of oxidation of the coal in the slurry could be determined from the current against time ( $I/t$ ) response for the oxidation of  $\text{Fe}^{2+}$  in the presence of coal [15]. The overall feasibility of the electrochemical oxidation of Alberta coal slurries was first investigated at room temperature and a typical response is shown in Fig. 3 (curve c). As seen from the graph, the current decreases with time of electrolysis. This decay of the current with time, as compared to the theoretical response in Fig. 3, curve b, when the  $\text{Fe}^{2+}$  is fully regenerated at all times, has been reported previously in the literature and has been attributed to the build-up of oxidized organic functionalities at the coal surface with time of electrolysis [9–13, 15, 17], thus leading to a poor efficiency of  $\text{Fe}^{2+}$  regeneration.

Since higher temperatures are known to yield higher

coal oxidation rates [11, 12], more extensive studies of the electrochemical oxidation of Alberta coals were carried out at  $90^\circ \text{C}$ . Typical  $I/t$  data obtained at  $90^\circ \text{C}$  and 1.0 V with respect to RHE are shown in Fig. 4 (curve a) for an experiment in which 6 g of Vesta coal (200 mesh) was oxidized in 120 ml of 1 M  $\text{H}_2\text{SO}_4$  containing 15 mM  $\text{FeSO}_4$ , together with the  $I/t$  data for the oxidation of 15 mM  $\text{FeSO}_4$  in the absence of any coal (curve b). The extent of the regeneration of  $\text{Fe}^{2+}$  by the reaction of coal with  $\text{Fe}^{3+}$  is clear from these curves, as curve a exhibits higher currents for a longer period of time as compared to curve b.

It should be noted that the absolute value of the oxidation current at any time depends on the coal:Fe ratio present in the slurry, as well as on the rate constant of the reaction. Three different ratios were utilized (in the range of 10.0 to 3.3 mg of coal per ml of solution per mM of  $\text{Fe}^{2+}$ ) in this study, so that a significant extent of oxidation could be achieved within a reasonable time period, e.g., 24 h. The  $I/t$  response during the electrochemical oxidation of Highvale coal for different coal:Fe ratios is shown in Fig. 5. It can be clearly seen from this figure that as the coal:Fe ratio increases, the current remains higher for a longer period of time. This is because the regeneration of  $\text{Fe}^{2+}$  becomes more efficient due to the availability of a greater number of active coal sites.

As seen in Figs 4 and 5, the current decreases fairly rapidly at short times (0–4 h), but then decreases more slowly at longer times (5–24 h). This behaviour is

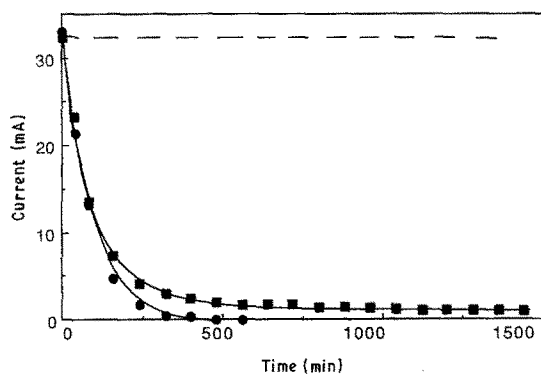


Fig. 3. Current response during the oxidation of 15mM  $\text{FeSO}_4$  at room temperature in 1 M  $\text{H}_2\text{SO}_4$  with a (●) no coal added, b (---) theoretical response when  $\text{Fe}^{2+}$  is fully regenerated, and c (■) with partial regeneration by 6 g of Highvale coal (200 mesh).

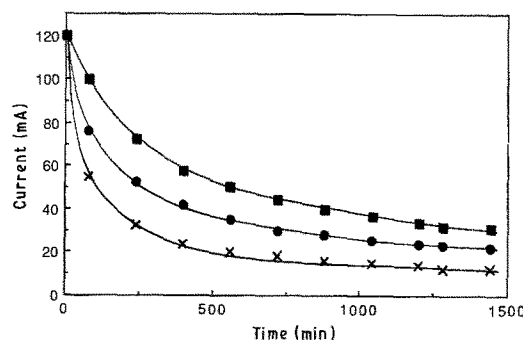


Fig. 5. Current response during the oxidation of Highvale coal (200 mesh) at  $90^\circ \text{C}$  for the following coal:Fe ratios. a (■) = 10.0 ( $150 \text{ mg ml}^{-1}$  coal + 15 mM  $\text{FeSO}_4$ ); b (●) = 6.6 ( $100 \text{ mg ml}^{-1}$  coal + 15 mM  $\text{FeSO}_4$ ); c (x) = 3.3 ( $50 \text{ mg ml}^{-1}$  coal + 15 mM  $\text{FeSO}_4$ ).

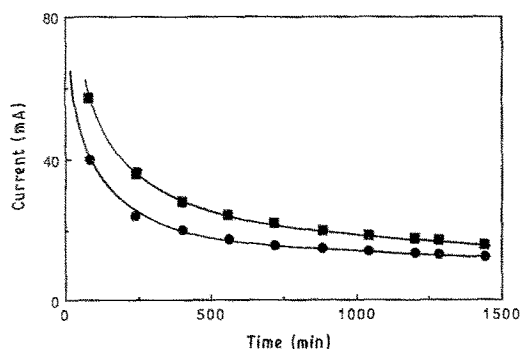


Fig. 6. Effect of particle size on the rate of electrochemical oxidation of Vesta coal at 90°C. (■) 200 mesh; (●) 60 mesh.

typical of that observed for all types of Alberta coals under study, as well as the previously reported loss of activity due to coal surface oxidation of various other coals [6–13, 15]. Since the current in Fig. 4 is equal to the rate of hydrogen production, the decrease of current with time is also indicative of a reduction in the rate of hydrogen production with electrolysis time.

The effect of coal particle size on the activity of the coal towards electrochemical oxidation is demonstrated in Fig. 6 for Vesta coal of two particle sizes, < 60 mesh (> 250  $\mu\text{m}$ ) and > 200 mesh (< 75  $\mu\text{m}$ ). As seen in the figure, the activity decreases as the coal particle size increases. This may be related directly to the decrease in the real surface area of the coal sample as the particle size increases.

**3.2.2. Kinetic analysis.** Several investigators [12–15, 23, 24] have attempted the kinetic analysis of the electrochemical oxidation data of coal slurries. These have involved assumptions of pseudo first order [11–13], second order [15, 24] and diffusion controlled [23] reaction mechanisms. For example, an apparent rate constant for the initial oxidation (only for  $\sim 6$  h) of a German coal (Westerholt) was obtained by Kreysa *et al.* [15], assuming second order reversible reaction kinetics. We have developed [19] a new graphical method for the analysis of the kinetics of the electrochemical oxidation of coal by  $\text{Fe}^{3+}$  species in acidic slurries, assuming second order irreversible reaction (first order with respect to both  $\text{Fe}^{3+}$  and coal) kinetics. Our approach is similar in some ways to that of Kreysa *et al.* [15], and yet a number of different assumptions and methods are involved.

In the electrochemical oxidation of coal mediated by  $\text{Fe}^{3+}$ , two oxidation reactions occur simultaneously. The oxidation of coal by  $\text{Fe}^{3+}$  (Reaction 1) results in the production of  $\text{Fe}^{2+}$ . The  $\text{Fe}^{2+}$  thus generated is then oxidized (Reaction 2) at the electrode at an applied potential of 1.0 V with respect to RHE in 1 M  $\text{H}_2\text{SO}_4$ . These two reactions proceed at different rates at all times of electrolysis.

The current which flows as Reaction 2 proceeds, measured as a function of time of electrolysis, contains information about both the concentration of  $\text{Fe}^{2+}$  ( $C_R$ ) in the slurry and its time derivative [15, 22]. The overall flux of  $\text{Fe}^{2+}$  at any time,  $t$ ,  $(dC_R/dt)_{\text{Total},t}$ , in the coal slurry during the electrolysis depends both on the

rate of coal oxidation (rate of generation of  $\text{Fe}^{2+}$ ) at  $t$ ,  $(dC_R/dt)_{\text{coal},t}$ , and the rate of electrochemical oxidation of  $\text{Fe}^{2+}$  (rate of consumption of  $\text{Fe}^{2+}$ ) at the anode at  $t$ ,  $(dC_R/dt)_{\text{ecl},t}$  and can be expressed as,

$$\left(\frac{dC_R}{dt}\right)_{\text{Total},t} = \left(\frac{dC_R}{dt}\right)_{\text{coal},t} - \left(\frac{dC_R}{dt}\right)_{\text{ecl},t} \quad (4)$$

Assuming second order kinetics, the rate of coal oxidation can also be expressed as,

$$\text{rate} = k_c C_o C_{\text{coal},t} \quad (5)$$

where  $k_c$  is the rate constant of the oxidation of coal by  $\text{Fe}^{3+}$ ,  $C_o$  is the concentration of the oxidant,  $\text{Fe}^{3+}$ , at the coal surface at  $t$ , and  $C_{\text{coal},t}$  is the concentration of the active coal sites at  $t$ . It is assumed that  $C_o$  is equal to the bulk  $\text{Fe}^{3+}$  concentration at all times of electrolysis. From this, the following expression was derived [19] to obtain the kinetic parameters

$$\frac{1}{(I_0 - I_t)} \left[ \left(\frac{dI}{dt}\right)_t + \left(\frac{k_c A}{V}\right) I_t \right] = k_c C_{\text{coal},o} - \frac{k_c}{zFV} \left[ Q_t - \frac{V(I_0 - I_t)}{k_c A} \right] \quad (6)$$

where  $k_c$  is the electrochemical mass transfer rate constant and is defined as the ratio of the diffusion coefficient of  $\text{Fe}^{2+}$  to the thickness of the diffusion-layer at the electrode surface (fixed by a constant stirring rate of the slurry).  $C_{\text{coal},o}$  represents the initial concentration of the active sites of the coal in a slurry of volume of  $V$  (litres),  $Q_t$  denotes the total charge passed at any  $t$ , while  $I_t$  represents the current at  $t$ . The value of  $z$  (the number of electrons involved in the complete oxidation of each site on the coal surface) is difficult to estimate due to the heterogeneous nature of the coal surface. Depending on the oxidation state of the carbon atoms of the active site,  $z$  could vary from 1 to 8 per carbon atom reacted. Kreysa *et al.* (11) have used a value of 2 for  $z$  for their mechanism of coal oxidation. However, the precise value is unknown and hence we have assumed  $z$  to be the same in each experiment and have taken it to be equal to 1 for ease of calculation. It should be noted that  $z$  and  $k_c$  are both unknowns in the  $k_c/zFV$  term in Equation 6. If  $z$  has another value, this will affect the absolute, but not the relative, magnitude of  $k_c$  determined in different experiments.

From a plot of  $1/(I_0 - I_t) [(dI/dt)_t + (k_c A/V)I_t]$  against  $[Q_t - V(I_0 - I_t)/k_c A]$ , the rate constant,  $k_c$ , can be determined from any electrolysis experiment. In Fig. 7, representative plots of this kind for Highvale coal are shown for two different coal particle sizes. It can be seen that two slopes are observed, leading to two rate constants,  $k_{c,1}$  and  $k_{c,2}$ , respectively. The presence of two rate constants indicates that the mechanism of the reaction is different in the initial stages of oxidation from that at longer times of electrolysis. As seen in the figure,  $x$ - and  $y$ -intercepts for the plots are higher for the small coal particle sizes than for the bigger ones. Large  $y$ -intercepts are indicative of a high concentration of active sites

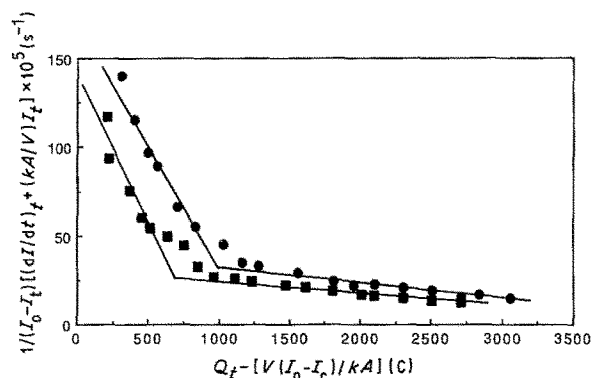


Fig. 7. Second order kinetics plots for the oxidation of 12g of Highvale coal at 1.0 V against RHE and 90°C in 1M H<sub>2</sub>SO<sub>4</sub>. (◆) 200 mesh; (■) 60 mesh.

originally exposed to the reaction media (Equation 6). Under identical experimental conditions, smaller particles are found to contain more of the  $k_{c,1}$  and  $k_{c,2}$  type sites than the larger particles for all the four types of coals studied. For example, 12 g of 200 mesh Highvale coal contain 0.09 and 0.4 mol l<sup>-1</sup>, respectively, of  $k_{c,1}$  and  $k_{c,2}$  type sites, while 12 g of the 60 mesh coal contains 0.08 and 0.3 mol l<sup>-1</sup>, respectively, of  $k_{c,1}$  and  $k_{c,2}$  type sites. It is also noteworthy that as the weight of the coal increases, the concentration of the  $k_{c,1}$  and  $k_{c,2}$  type sites also increases proportionally, indicating the validity of the method of kinetic analysis.

The rate constants obtained for the oxidation of the four Alberta coals (200 and 60 mesh) studied are given in Table 2, along with a number of selected properties [25, 26] of these coals. As stated above, the value of  $k_c$  depends on the assumed value of  $z$ . Any change in  $z$  will correspondingly change  $k_c$ . Therefore, the relative  $k_c$  values would not be affected if a different  $z$  value had been assumed. It is seen from Table 2 that, generally, both  $k_{c,1}$  and  $k_{c,2}$  increase in the order of Vesta < Bow City < Highvale in the sub-bituminous rank, while the bituminous Luscar–Sterco Coal Valley coal has a higher activity than the sub-bituminous coals, except for Coal Valley coal, for reasons which are unknown at present.

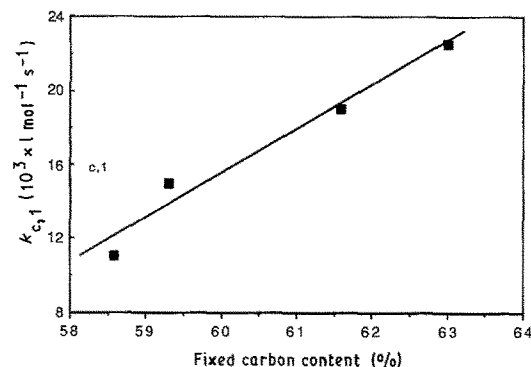


Fig. 8. Electrochemical coal oxidation rate constant ( $k_{c,1}$ ) as a function of fixed carbon content of the coal.

The rate constants reported in Table 2 are generally similar in magnitude to those reported in the literature. Kreysa *et al.* [15] reported a rate constant of  $2.25 \times 10^{-3} \text{ mol}^{-1} \text{ s}^{-1}$  for the initial stages of the oxidation of Westerholt coal at 70°C. Kawakami *et al.* [24] have reported two rate constants,  $k_1 = 3.89 \times 10^{-3} \text{ s}^{-1}$  and  $k_2 = 1.27 \times 10^{-4} \text{ s}^{-1}$ , respectively, for the oxidation of Illinois No. 6 coal (200  $\mu\text{m}$ ) at 40°C. Assuming a pseudo first order reaction mechanism, Dhooze and Park [11] have determined a rate constant of  $3.7 \times 10^{-5} \text{ s}^{-1}$  at 20°C for the oxidation of sub-bituminous San Juan coal. Lalvani [23] has reported a rate constant of  $2.23 \times 10^{-4} \text{ s}^{-1}$  for the oxidation of North Dakota lignite coal, also assuming pseudo first order (mass transfer rate limited) kinetics.

Table 2 shows that the sequence of the electrochemical activity of the coals is parallel to their fixed carbon (FC) content\*, as demonstrated in Fig. 8. As seen in the figure, a reasonable correlation can be drawn between the rate constant of a coal obtained from mediated electrochemical oxidation and its fixed carbon content. However, a detailed study of the activity of coals of a wide range of ranks towards electrochemical oxidation is necessary in order to make a firm conclusion about the correlation.

The fixed carbon content and calorific value of a coal are generally accepted as key criteria for deter-

Table 2. Electrochemical rate constants for the oxidation of Alberta coals by Fe<sup>3+</sup> (and related data) at 90°C

Coal type (origin)	Rate constants† (l mol <sup>-1</sup> ) × 10 <sup>3</sup>		Fixed carbon‡ (%)	Volatile matter‡ (%)
	$k_{c,1}$	$k_{c,2}$		
Coal Valley	22 (12.0)	1.4 (0.8)	63.0	37.0
Highvale	19 (18)	0.9 (0.8)	61.6	38.4
Bow City	15 (12.0)	0.8 (0.7)	59.3	40.7
Vesta	11 (8.0)	0.6 (0.5)	58.6	41.4

† values without parentheses are for 200 mesh; those in parentheses are for 60 mesh.

‡ dry ash free, measured for the pretreated coal samples.

\* Fixed carbon content of the coals studied were determined after subjecting them to a pretreatment process.

mining coal rank [30, 31]. However, many other properties of coal such as reflectance [26, 32], aromaticity [30], etc., are utilized to determine coal rank. As the electrochemically measured rate constants for the oxidation of coal have been shown to vary with the FC content, it is possible that electrochemical activity could be used as another indicator of coal rank. This is further supported by the fact that the electrochemical rate constants decrease as the volatile matter content of the coal increases, as seen in Table 2.

From the plots of Fig. 7,  $C_{\text{coal,o}}$  can be determined from the  $y$ -intercepts, which can then yield the total charge,  $Q_c$ , obtainable from any coal sample by its exhaustive oxidation. For example,  $Q_c$  obtained from the extrapolation of the slopes for a typical electrolysis experiment in which 6 g of Highvale (200 mesh) coal were oxidized for 24 h in the presence of 15 mM  $\text{FeSO}_4$  was calculated to be  $\sim 2800$  C assuming  $z = 1$ . The total charge passed in an experiment conducted under identical conditions, but for 65 h, was found to be  $\sim 3800$  C, i.e., higher than the predicted maximum  $Q_c$ . Also, a considerable degree of electrochemical activity still remains after 65 h of electrolysis.

These results indicate that after prolonged periods of electrolysis, the simplistic view of coal oxidation proposed above may need modification. It is likely that as the coal surface becomes more oxidized with time,  $C_{\text{coal,o}}$  begins to increase as sites beneath the surface become accessible to oxidation by  $\text{Fe}^{3+}$ , i.e. the coal surface area available for electrochemical oxidation increases with time. It is also feasible that as the oxidation reaction proceeds, the coal particles may crack, exposing new oxidizable sites to solution, thereby also increasing  $C_{\text{coal,o}}$  with time. It is also possible that the  $z$  value changes at some sites at long times of oxidation. Both of these processes would be highly desirable and would make the coal more active to electrochemical oxidation than anticipated, perhaps even resulting in eventual total oxidation.

*3.2.3. Analysis of the products of electrochemical oxidation of Alberta coal slurries.* The gaseous products obtained during the electrochemical oxidation of coal in Fe-containing 1 M  $\text{H}_2\text{SO}_4$  slurries were analyzed at regular intervals during the electrolysis experiments. The primary gaseous product obtained from the anode compartment of the electrolysis cell was  $\text{CO}_2$ , as has been the case for most of the coals examined in earlier studies [9, 11, 12, 14, 15, 17]. The rate of production of  $\text{CO}_2$  was determined by GC as a function of time in most electrolysis experiments. It was generally observed that, after the first 5 to 6 h of electrolysis, the rate of  $\text{CO}_2$  production reached a steady-state value which remained essentially constant until the end of the experiment.

In Fig. 9, the rate of  $\text{CO}_2$  production during the electrochemical oxidation of the four types of Alberta coals is presented. As can be seen from the figure, Highvale, Bow City and Coal Valley coals produce smaller amounts of  $\text{CO}_2$  than does Vesta coal. This may indicate that Vesta coal is different from the other

coals in terms of the nature of its surface active sites, in that it may contain more functional groups which can be readily oxidized to  $\text{CO}_2$  by  $\text{Fe}^{3+}$ . It should be noted that Vesta is a sub-bituminous C coal, while the other coals are all sub-bituminous B or bituminous [25]. Also, a relatively large inertinite (charred plant tissue) content [25, 32] is a distinguishing feature of Vesta coal. Its presence could alter the mechanism of oxidation of the coal by  $\text{Fe}^{3+}$  and lead to particularly high yields of  $\text{CO}_2$  during electrochemical oxidation.

The current efficiency of  $\text{CO}_2$  production was estimated by assuming that an average of four electrons are required per  $\text{CO}_2$  molecule produced. This efficiency is in the range of ca. 30–40% at electrolysis times less than  $\sim 2$  to 3 h, while higher efficiencies ( $\sim 80\%$ ) are obtained after about 15 h of electrolysis (Fig. 10) for all of the coals studied. This apparent change in the efficiency of  $\text{CO}_2$  production could imply that at short times, a greater proportion of the charge is utilized in the formation of solution-soluble products and/or high oxidation state surface-based functionalities than in  $\text{CO}_2$  production [11, 12, 14, 15, 17], as compared to the reaction at longer times.

It is also possible that the average oxidation state of the carbon atoms in the coal increases with time of electrolysis. This would imply that the reaction mechanism changes with time of electrolysis, which is consistent with the presence of two rate constants in Fig. 8. In fact, both of these interpretations of the increasing  $\text{CO}_2$  yield with electrolysis time are related, in that both require a change in the reaction pathway with time of electrochemical oxidation, consistent with the results of the kinetic analysis [19]. A concomitant periodic analysis of the coal surface using FTIR and XPS, and of the solution products, would be helpful in more fully interpreting the changing  $\text{CO}_2$  production current efficiencies with time. The analysis of the coal surface could also aid in deducing the oxidation state of carbon at the reactive sites with time of oxidation.

The current efficiency for the production of  $\text{CO}_2$  during the electrochemical oxidation of coals has been reported by several research groups. In their studies with US anthracite coals, Okada *et al.* [9] determined the initial current efficiency for the production of  $\text{CO}_2$  at  $80^\circ\text{C}$  to be about 5%, rising to 10% after 15 h of electrolysis. Dhooge and Park [12] reported a current efficiency of 15–30% at  $20^\circ\text{C}$  and 30–50% at  $70^\circ\text{C}$  for San Juan (sub-bituminous) coal in 1 M  $\text{H}_2\text{SO}_4$  solutions, also assuming four electrons per  $\text{CO}_2$  molecule produced. These studies clearly show that the current efficiency of  $\text{CO}_2$  production depends on such experimental factors as the temperature of the reaction media, the rank and other properties of the coal, as well as the assumed number of electrons required to form  $\text{CO}_2$  from coal.

### 3.3. Possible mechanisms of electrochemical oxidation of coal slurries

*3.3.1. Structural model.* A three dimensionally cross-linked, highly porous, macromolecular structure of

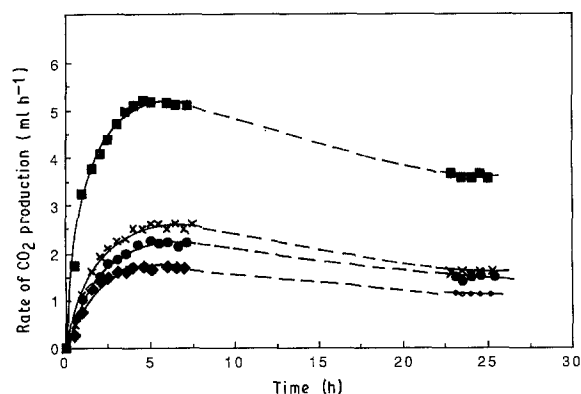


Fig. 9. Rate of production of  $\text{CO}_2$  with time of electrolysis of 6 g of 200 mesh coal + 15 mM  $\text{FeSO}_4$  at  $90^\circ\text{C}$ . (■) Vesta, (●) Bow City, (x) Highvale, and (◆) Luscar-Sterco Coal Valley coal. Note: no  $\text{CO}_2$  production data was taken during the time indicated by the dashed lines.

coal has been well established in the literature [33–35]. One view of the details of this structure is to consider that a number of different types of reactive sites (RS), which are susceptible to oxidative attack, are present. These reactive sites have been suggested [35] to be located in three different general areas of coal, i.e. at the external surface of the coal (*type 1*), at internal pore surfaces (*type 2*) and within the solid coal matrix (*type 3*). These possibilities are represented schematically in Fig. 11.

It can be suggested that the kinetics of coal oxidation by  $\text{Fe}^{3+}$  would be influenced by the varying accessibility of  $\text{Fe}^{3+}$  to these different reactive sites, resulting in different rate constants for oxidation of the different sites. Functional groups present at the external coal surface (*type 1*) might be expected to react readily with  $\text{Fe}^{3+}$ , as compared to those located at less accessible sites (*types 2 and 3*). The rate of reaction of  $\text{Fe}^{3+}$  with *type 1* sites should be determined primarily by the initial outer coal surface area, whereas the reaction rate with *type 2* sites would be more dependent on such factors as the size of the pore openings, etc. The rate of reaction with *type 3* sites would depend on the ability of  $\text{Fe}^{3+}$  to penetrate the coal matrix.

Previous studies [5, 13–15, 17, 36] of the electrochemical oxidation of coal by  $\text{Fe}^{3+}$  have indicated the formation of oxidized organic moieties at the outer coal, surface with time of electrolysis. FTIR studies

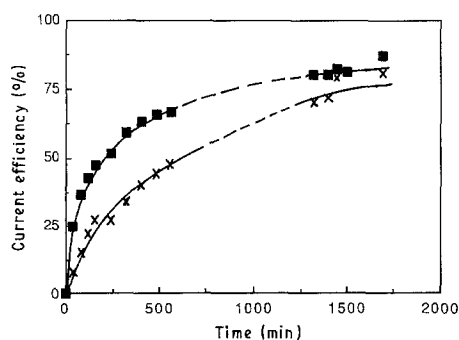


Fig. 10. Current efficiency of  $\text{CO}_2$  production, assuming 4 electrons required per  $\text{CO}_2$  molecule generated, during the oxidation of 6 g of 200 mesh coal + 15 mM  $\text{FeSO}_4$  in 1 M  $\text{H}_2\text{SO}_4$  at  $90^\circ\text{C}$ . (■) Vesta; (x) Highvale. Note: current efficiency data were not available for the time period indicated by dashed line.

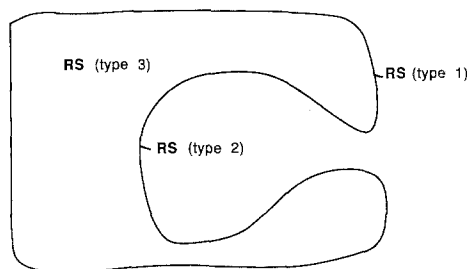


Fig. 11. Schematic diagram showing the possible different locations of reactive sites (RS) of coal particles.

[37] carried out in our laboratory have also indicated the oxidation of surface functional groups. These observations clearly imply that at short times, a significant portion of the reaction of coal with  $\text{Fe}^{3+}$  must take place at the exposed coal surface (*type 1* sites), as perhaps depicted by the rate constant ( $k_{c,1}$ ) obtained at short times ( $< 10$  h) of electrolysis.

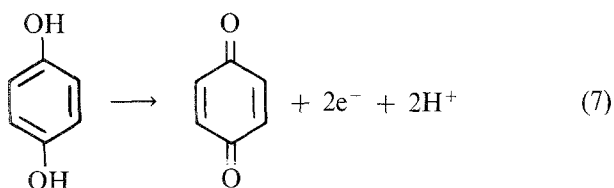
At longer times ( $> 10$  h) of electrolysis, a second lower rate constant,  $k_{c,2}$ , is observed. It is possible that at longer times of electrolysis, the functional groups present at *type 2* sites become more accessible to  $\text{Fe}^{3+}$  while *type 1* sites continue to be depleted. The rate of the coal oxidation reaction ( $k_{c,2}$ ) may then become more influenced by the rate at which  $\text{Fe}^{3+}$  accesses these sites and by the rate at which the reaction products leave the pores of the coal.

Reaction with *type 3* sites may occur after prolonged electrochemical oxidation. *Type 3* sites may also become exposed by the cracking of the coal particles, thus converting them to *type 1* or *2* sites, equivalent to the observed increase in  $C_{\text{coal},o}$  with time.

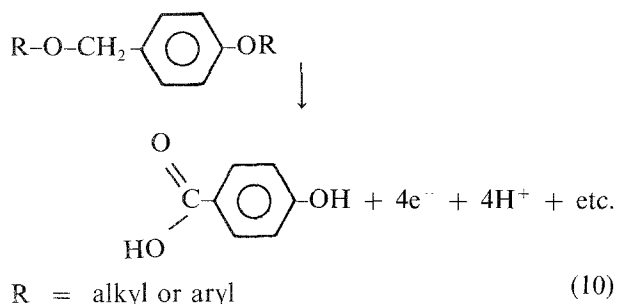
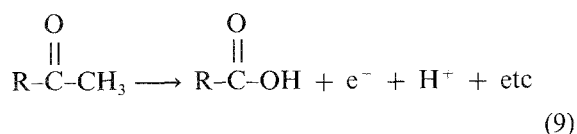
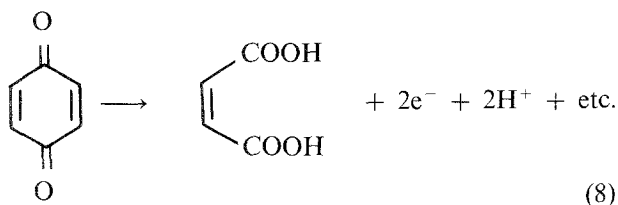
**3.3.2. Functional group model.** The fact that two different rate constants are observed with long time of electrochemical oxidation of coal may also be related to the oxidation of a range of organic functional groups at the coal surface, including phenols, hydroxyls, carbonyls, carboxyls, acyls, etc. The rate of oxidation of coal by  $\text{Fe}^{3+}$  in acidic media is likely to depend on the relative susceptibility of the various functional groups present on the coal surface to oxidative attack. These functional groups would be expected to have different formal redox potentials and would therefore undergo oxidation by  $\text{Fe}^{3+}$  at different rates. Based on previous electrochemical studies not related directly to coal materials [38], numerous organic functional groups can be singled out which might be expected to undergo oxidation at potentials less positive than the formal potential of  $\text{Fe}^{3+}$  in 1 M  $\text{H}_2\text{SO}_4$ . For example, functional groups such as hydroquinones, phenols, aromatic amines and organosulphur compounds are likely to be oxidizable at potentials lower than those required for the oxidation of aromatic hydrocarbons, carboxyls and heterocyclic compounds [39].

With this model, it is possible that  $k_{c,1}$  depicts the  $\text{Fe}^{3+}$  mediated oxidation of coal surface sites having a relatively low formal potential (for example, the oxidation of hydroxyl to carbonyl species,  $E^{\circ'} = 0.69$  V with respect to SHE), as shown in Reaction 7.



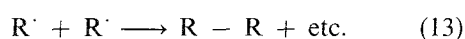
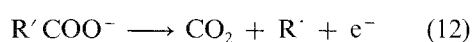
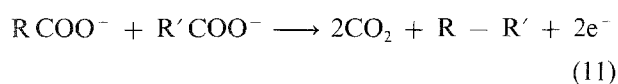


As these sites are consumed, higher oxidation states are produced and other oxidation reactions could occur, resulting in the formation of various carboxylic acids. Also, other coal sites having more positive formal redox potentials may gradually become exposed and react with  $\text{Fe}^{3+}$ , as demonstrated in Reactions 8 to 10 (in each reaction, the electrons are provided by  $\text{Fe}^{3+}$ ).



The rates of these reactions (given by  $k_{c,2}$ ) are expected to be lower than the rate of the earlier oxidation reactions depicted by  $k_{c,1}$ , as the electrochemical driving force, i.e., the overpotential, equivalent to the difference in the potentials of the redox reaction and that of  $\text{Fe}^{3+/2+}$ , is now likely to be lower.

This functional group interpretation of the observed kinetics of the long-time electrochemical oxidation of coal slurries would be consistent with the relatively low current efficiency for  $\text{CO}_2$  production observed during the time scale when  $k_{c,1}$  is observed, and the higher current efficiency of  $\text{CO}_2$  production at longer times of oxidation (in the range of  $k_{c,2}$ ). This is because the majority of the oxidation reactions are expected to ultimately lead to the production of  $\text{CO}_2$  by Kolbe-type reaction processes [5, 39], as shown in Reactions 11 to 13,



where  $\text{R}'$  is an alkyl free radical and R and  $\text{R}'$  are two different alkyl fractions.

Due to the porous and complex nature of coal, it is unreasonable to expect that a single structural or compositional model of the oxidation of coal by  $\text{Fe}^{3+}$  can adequately explain the kinetic results obtained. Instead, a hybrid model involving the oxidation of various functional groups which are located in a range of sites of varying accessibility to  $\text{Fe}^{3+}$  and having variable abilities to allow the escape of the oxidation products, would be more appropriate. It is possible that the nature of the functional groups being oxidized is more important at short times of reaction, while, at long times, the accessibility of sites may dominate the oxidation kinetics.

#### 4. Conclusions

The electrochemical oxidation of four different types of Alberta coals of bituminous and sub-bituminous rank by  $\text{Fe}^{3+}$  was studied in 1 M  $\text{H}_2\text{SO}_4$  at  $90^\circ\text{C}$ . Two different particle sizes (60 and 200 mesh) were used in this work. A kinetic analysis of the  $I/t$  data revealed two rate constants,  $k_{c,1}$  and  $k_{c,2}$ , representative of the initial (6 h) and subsequent (6 to 24 h) stages of coal oxidation, respectively. The sequence of coal activity, as determined by the rate constants, are in the order of Highvale > Bow City > Vesta, while Coal Valley coal showed a higher activity than the other three sub-bituminous coals. These rate constants were found to decrease as the fixed carbon content of the coals decreases, consistent with the decrease in the rank of the coal.

Gaseous products evolved from the coal slurry chamber were analyzed by chromatographic methods and  $\text{CO}_2$  was the only product detected. The rate of production of  $\text{CO}_2$  as a function of oxidation time was found to reach a steady-state within  $\sim 6$  h of electrolysis. The current efficiency for the production of  $\text{CO}_2$  was found to be under 40% up to  $\sim 3$  h of electrolysis and 70 to 80% after  $\sim 22$  h of electrolysis.

Structural and functional group models of coal oxidation have been presented in an effort to explain the observed kinetic behaviour and products of the electrochemical oxidation of Alberta coals in acidic slurries.

#### Acknowledgements

This research was partially funded by a grant-in-aid of research from the Alberta/Canada Energy Resources Research Fund, jointly established by the Government of Canada and by the Government of Alberta and administered by the Alberta office of Coal Research and Technology. Financial assistance from the Natural Sciences and Engineering Research Council of Canada is also gratefully acknowledged. We also acknowledge P. Demcoe for useful discussions, and M. Benn, for the use of the chromatographic equipment.

## References

- [1] C. S. Lynch and A. R. Collett, *Fuel* **11** (1932) 408.
- [2] R. Eddinger and D. Demorest, *ibid.* **26** (1947) 157.
- [3] R. Belcher, *J. Soc. Chem. Ind. Lond.* **67** (1948) 213, 217, 218, 265, 267.
- [4] M. H. Khumdkar and M. M. Kamal, *Fuel* **45** (1966) 9.
- [5] R. W. Coughlin and M. Farooque, *Nature* **279** (1979) 301.
- [6] M. Farooque and R. W. Coughlin, *ibid.* **280** (1979) 666.
- [7] *Idem Fuel* **58** (1979) 705.
- [8] *Idem J. Appl. Electrochem.* **10** (1980) 729.
- [9] G. Okada, V. Guruswamy and J. O'M. Bockris, *J. Electrochem. Soc.* **128** (1981) 2097.
- [10] R. P. Baldwin, K. T. Jones, J. T. Joseph and J. L. Wong, *Fuel* **60** (1981) 739.
- [11] P. M. Dhooge, D. E. Stilwell and S. M. Park, *J. Electrochem. Soc.* **129** (1982) 1719.
- [12] P. M. Dhooge and S. M. Park, *ibid.* **130** (1983) 1029.
- [13] K. E. Anthony and H. G. Linge *ibid.* **130** (1983) 2217.
- [14] P. M. Dhooge and S. M. Park, *ibid.* **130** (1983) 1539.
- [15] G. Kreysa and W. Kochanek, *ibid.* **132** (1985) 2084.
- [16] O. J. Murphy, J. O'M. Bockris and D. W. Later, *Int. J. Hydrogen Energy* **10** (1985) 453.
- [17] S. M. Park, *J. Electrochem. Soc.* **131** (1984) 363C.
- [18] J. D. Campbell and M. P. du Plessis, Report no. YCLQ-2, Coal Research Department, Alberta Research Council, Edmonton, Alberta, Canada (1982).
- [19] G. Thomas, S. Whitcombe, M. Farebrother and V. I. Birss, in press.
- [20] G. Thomas, M. Chettiar and V. I. Birss, (submitted to *J. Electrochem. Soc.*)
- [21] *Idem*, (submitted to *J. Electrochem. Soc.*)
- [22] A. J. Bard and L. R. Faulkner, in 'Electrochemical Methods', John Wiley & Sons, New York (1980) Chapters 8, 10 and 11.
- [23] S. B. Lalvani, *Chem. Eng. Commun.* **48** (1986) 117.
- [24] K. Kawakami, T. Okumura, K. Kusunoki, K. Kusakabe, S. Morooka and Y. Kato, *J. Chem. Eng. Jpn.* **19** (1986) 134.
- [25] S. Parkash, S. K. Chakrabarty and M. P. du Plessis, Coal Report 84-2, Coal Research Department, Alberta Research Council, Edmonton, Alberta, Canada (1984).
- [26] S. Parakash, M. P. du Plessis, A. R. Cameron and W. D. Kalkreuth, *Int. J. Coal Geol.* **4** (1984) 209.
- [27] V. Valković, Trace Elements in Coal, (1983) CRC Press Inc., Boca Raton, Florida.
- [28] R. Bauwman and I. L. C. Freriks, *Fuel* **59** (1980) 315.
- [29] B. C. Gerstein, P. D. Murphy and L. M. Ryan, in 'Coal Structure', (edited by R. A. Meyers), Academic Press, New York (1982) Chapter 4.
- [30] F. P. Miknis, M. J. Sullivan, V. J. Bartuska and G. F. Maciel, *Org. Geochem.* **3** (1981) 19.
- [31] D. A. Axelson, in 'Solid State Nuclear Magnetic Resonance of Fossil Fuels', Polyscience Publications, Montreal (1985) Chapter 7.
- [32] W. J. Montgomery, in 'Analytical Methods for Coal and Coal Products', (edited by C. Karr, Jr.), Academic Press, New York (1978) Vol. 1, Chapter 6.
- [33] R. A. Meyers (ed.), 'Coal Structure', Academic Press, New York (1982) Chapter 2.
- [34] W. R. Grimes, in 'Coal Science', (edited by M. L. Gorbaty, J. W. Larsen and I. Wender), Academic Press, New York (1982) Vol. 1, Chapter 2.
- [35] J. W. Larsen, T. K. Green, P. Choudhury and E. W. Kuemmerle, in 'Coal Structure', (edited by M. L. Gorbaty and K. Ouchi) Adv. in Chem., Series 192, Am. Chem. Soc., Washington DC (1981) Chapter 18.
- [36] D. W. Krevelen, in 'Coal', Elsevier, New York (1961) Chapter 23.
- [37] A. Pomfret, C. Gibson, K. D. Bartle, N. Tyler and D. G. Mills, *Fuel Processing Technology* **10** (1985) 239.
- [38] V. I. Birss, G. Thomas and M. Chettiar, Final Report, 'Electrolysis of Alberta Coal Slurries', Alberta Office of Coal Research and Technology, Report Bo. 2835-RG-85/9, Edmonton, Alberta (1988).
- [39] M. R. Rifi and F. H. Covitz, in 'Introduction to Organic Electrochemistry', Marcel Dekker, New York (1974) p. 395.
- [40] L. Ebersson, in 'Organic Electrochemistry', (edited by M. M. Baizer) Marcel Dekker, New York (1973) Chapter 13.